



HAL
open science

Tethering of hexokinase 2 to mitochondria promotes resistance of liver cancer cells to natural killer cell cytotoxicity

Anne Aublin-gex, Florentine Jacolin, Olivier Diaz, Clémence Jacquemin, Antoine Marçais, Thierry Walzer, Vincent Lotteau, Pierre-olivier Vidalain, Laure Perrin-cocon

► To cite this version:

Anne Aublin-gex, Florentine Jacolin, Olivier Diaz, Clémence Jacquemin, Antoine Marçais, et al.. Tethering of hexokinase 2 to mitochondria promotes resistance of liver cancer cells to natural killer cell cytotoxicity. *European Journal of Immunology*, 2024, 10.1002/eji.202350954 . hal-04781217

HAL Id: hal-04781217

<https://hal.science/hal-04781217v1>








Submitted on 13 Nov 2024

HAL is a multi-disciplinary open access archive for the deposit and dissemination of scientific research documents, whether they are published or not. The documents may come from teaching and research institutions in France or abroad, or from public or private research centers.

L'archive ouverte pluridisciplinaire **HAL**, est destinée au dépôt et à la diffusion de documents scientifiques de niveau recherche, publiés ou non, émanant des établissements d'enseignement et de recherche français ou étrangers, des laboratoires publics ou privés.

Research Article

Tethering of hexokinase 2 to mitochondria promotes resistance of liver cancer cells to natural killer cell cytotoxicity

Anne Aublin-Gex¹ , Florentine Jacolin¹, Olivier Diaz¹ ,
Clémence Jacquemin¹, Antoine Marçais² , Thierry Walzer² ,
Vincent Lotteau¹ , Pierre-Olivier Vidalain¹  and Laure Perrin-Cocon¹ 

¹ CIRI, Centre International de Recherche en Infectiologie, Team Viral Infection, Metabolism and Immunity, Univ Lyon, Inserm, U1111, Université Claude Bernard Lyon 1, CNRS, UMR5308, ENS de Lyon, Lyon, France

² CIRI, Centre International de Recherche en Infectiologie, Team Lymphocyte activation and signaling, Univ Lyon, Inserm, U1111, Université Claude Bernard Lyon 1, CNRS, UMR5308, ENS de Lyon, Lyon, France

Hexokinases (HKs) control the first step of glucose catabolism. A switch of expression from liver HK (glucokinase, GCK) to the tumor isoenzyme HK2 is observed in hepatocellular carcinoma progression. Our prior work revealed that HK isoenzyme switch in hepatocytes not only regulates hepatic metabolic functions but also modulates innate immunity and sensitivity to Natural Killer (NK) cell cytotoxicity. This study investigates the impact of HK2 expression and its mitochondrial binding on the resistance of human liver cancer cells to NK-cell-induced cytotoxicity. We have shown that HK2 expression induces resistance to NK cell cytotoxicity in a process requiring mitochondrial binding of HK2. Neither HK2 nor GCK expression affects target cells' ability to activate NK cells. In contrast, mitochondrial binding of HK2 reduces effector caspase 3/7 activity both at baseline and upon NK-cell activation. Furthermore, HK2 tethering to mitochondria enhances their resistance to cytochrome c release triggered by tBID. These findings indicate that HK2 mitochondrial binding in liver cancer cells is an intrinsic resistance factor to cytotoxicity and an escape mechanism from immune surveillance.

Keywords: Cytotoxicity · Hexokinase 2 · Mitochondria · NK cells · Tumor cell resistance



Additional supporting information may be found online in the Supporting Information section at the end of the article.

Introduction

Liver cancer is the fifth most common cancer and the fourth leading cause of cancer-related deaths in the world, with rising inci-

dence (www.iarc.fr) [1]. Hepatocellular carcinoma (HCC) represents a majority of primary malignant liver tumors, usually developing in the context of chronic liver disease. The liver is naturally infiltrated with innate lymphoid cells (ILCs) including natural killer (NK) cells that play a prominent role in the antitumoral defense. However, the tumor microenvironment shapes ILCs infiltrate in patients with HCC and several findings highlighted a reduced NK cells cytotoxic activity in the tumor [2–4]. There is

Correspondence: Dr. Laure Perrin-Cocon
e-mail: laure.perrin@inserm.fr

© 2024 The Author(s). *European Journal of Immunology* published by Wiley-VCH GmbH.

www.eji-journal.eu

This is an open access article under the terms of the Creative Commons Attribution-NonCommercial-NoDerivs License, which permits use and distribution in any medium, provided the original work is properly cited, the use is non-commercial and no modifications or adaptations are made.

a lower risk of recurrence [5] upon high infiltration with immune effector cells such as T cells, CD8⁺ T cells, $\gamma\delta$ T cells, and NK cells and a positive correlation between the density of infiltrating intra-tumoral NK cells and overall survival of patients [6]. Hence, advanced-stage HCC are often poorly infiltrated with NK cells that are also functionally impaired [7]. Overall, available data indicate that the tumor microenvironment can control ILC infiltrate and point toward dysfunctional NK cells in HCC. In addition, HCC cells are known to be resistant to NK-cell-mediated lysis [8–11]. This is linked to a decreased expression of some NK cell ligands [8, 9] but other mechanisms could also contribute to this resistance, and deciphering them would be instrumental to the development of new therapies.

NK cells induce target cell apoptosis via the release of cytotoxic granules containing perforin and granzymes and by binding death receptor ligands such as FasL and TRAIL. This cytotoxic function can be modulated by cytokines (such as IL-2, IL-12, IL-15, and IL-18) and a panel of ligands expressed by target cells [12]. Indeed, NK-cell degranulation is regulated by both activating and inhibitory receptors, their relative engagement allowing NK cells to discriminate normal from abnormal cells [13]. Healthy cells express MHC class I molecules that engage inhibitory receptors (KIR in humans) and are thus spared from NK cell activity. In contrast, transformed cells often express reduced levels of MHC molecules thus exposing them to NK cell action. Moreover, various stresses result in enhanced expression of ligands for NK activating receptors, such as the NKG2D ligands MICA/B and ULBPs [14]. Thus, understanding the modulation of NK cell activation and effector function is of major interest for the development of NK cell-based immunotherapies against cancer. NKG2D-dependent elimination of tumor cells has been documented in syngeneic mouse models of transplanted tumors [15]. In addition, adhesion molecules such as ICAM-1, Nectins, and Nectin-like molecules (i.e. PVR/CD155) often expressed on tumor cells promote the establishment of the killer synapse [16, 17] and modulate NK-cell activation and function by their interactions with several NK-cell receptors [18]. Moreover, increasing amounts of data indicate that bioenergetic metabolism modulates NK-cell differentiation and activity [19–21]. How metabolic changes associated with cellular transformation influence the susceptibility of tumor cells to cytolysis by NK cells is largely unknown.

Hexokinases (HK) control the first rate-limiting step of glucose catabolism by phosphorylating glucose to glucose-6-phosphate (G6P), fueling glycolysis as well as glycogen, pentose phosphate, and triglyceride synthesis. The human genome contains five genes, named HK1, HK2, HK3, Glucokinase (GCK), and HKDC1, encoding hexokinase isoenzymes with distinct enzymatic parameters and tissue distributions. GCK is a liver HK highly expressed in normal hepatocytes. Because it has a pseudo-allosteric response to glucose concentration, it plays a key role in the regulation of glucose metabolism by the liver and in the control of glycemia. Conversely, hexokinase 2 (HK2) has a high affinity for glucose and exhibits a high enzymatic activity even at low glucose concentrations. It is expressed in proliferating cells and activated immune cells such as dendritic cells to support their maturation by enhanc-

ing glycolytic activity [22]. HK2 is also overexpressed in many types of tumor cells, including HCC, to sustain their proliferation at low glucose concentrations. Indeed, during the cancerous transformation of hepatocytes, the liver hexokinase GCK is replaced by the “cancer-type” isoenzyme HK2 whose expression has been correlated with disease progression and the dedifferentiation of HCC cells [23]. HK2 expression is also inversely correlated to that of GCK in tumor lesions and is associated with poor overall survival [8]. When HK2 is artificially knocked down in HCC cell lines, glycolysis is repressed, and tumorigenesis is inhibited while cell death increases [24]. Consequently, HK2 induction has been proposed as a risk marker for HCC [25].

In addition to glucose phosphorylation, HKs have nonenzymatic roles often referred to as moonlighting functions. This suggests that the GCK-to-HK2 isoenzyme switch that characterizes HCC development has broader consequences than initially suspected with reported effects on autophagy, cell migration, and immunity [26–29]. To study the effect of the GCK-to-HK2 switch on HCC cell functions and phenotype, we replaced HK2 expression with GCK in Huh7 cells [8]. The replacement of HK2 by GCK rewired central carbon metabolism and restored some essential metabolic functions of normal hepatocytes such as lipogenesis, lipoprotein secretion, and glycogen storage [8]. We discovered that HK isoenzyme expression not only controls hepatic metabolic functions but also interferes with the intrinsic innate immunity of hepatocytes and antitumor immune surveillance. In particular, we showed that the replacement of HK2 by GCK in Huh7 HCC cells increased their sensitivity to NK cell cytolysis [8]. This suggests that HK2 expression promotes the escape of HCC cells from the immune response, but the underlying mechanisms have yet to be determined.

Unlike GCK, HK2 has a 10 amino acids N-terminal mitochondrial binding domain that binds the voltage-dependent anion channel (VDAC) protein [30]. This interaction tethers HK2 to the mitochondrial surface. In different cellular models, HK2 binding to mitochondria was reported to regulate the mitochondrial permeability transition pore and to have consequences on cellular metabolism, immune response, and sensitivity to apoptosis-inducing drugs [31]. Here, we thus explored the role of HK2 expression and its binding to mitochondria in the sensitivity of HCC cells to cytolysis by NK cells. Our results unraveled a mechanism of resistance in cells expressing HK2 linked to the ability of this enzyme to bind to the mitochondria.

Results

Replacing HK2 by GCK in human liver tumor cells confers susceptibility to cytolysis by NK cells

Huh7 and Huh6 are cancer cell lines derived from primary liver tumors and as such, they express HK2 but not GCK (ref. [8] for Huh7 and Supporting Information Fig. S1 for Huh6). We previously reported that Huh7 cells engineered to express GCK instead of HK2 are more susceptible to cytolysis by purified, primary NK

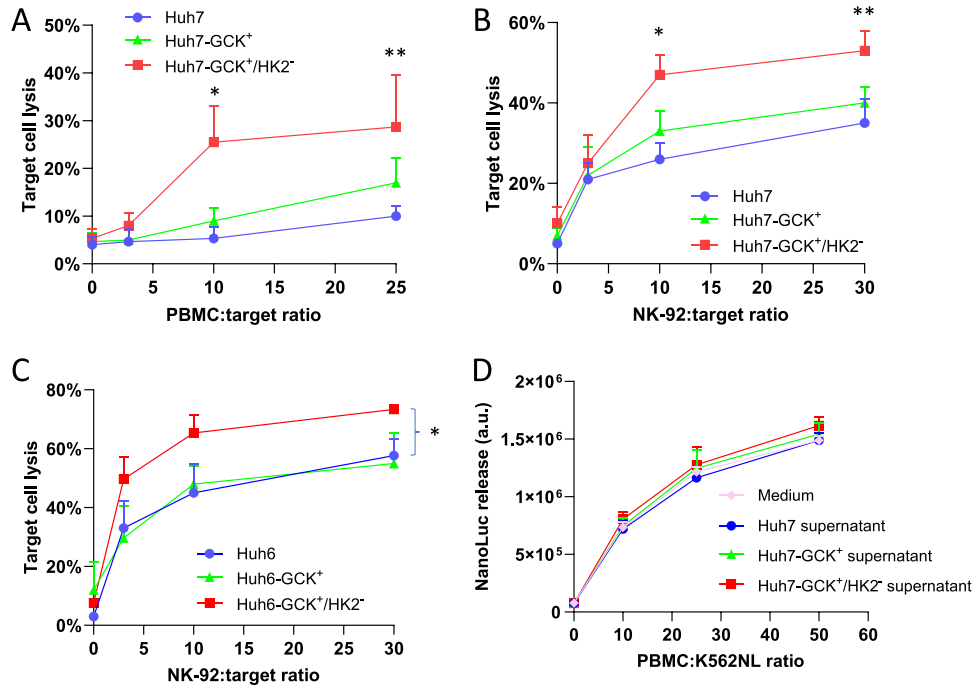


Figure 1. Susceptibility to NK cell-mediated cytotoxicity of Huh7 cells expressing HK2 and/or GCK. Huh7, Huh7-GCK⁺ or Huh7-GCK⁺/HK2⁻ (A, B) or Huh6, Huh6-GCK⁺ or Huh6-GCK⁺/HK2⁻ (C) were labeled with CTV and seeded. After 24 h, IL-2-preactivated PBMCs (A) or NK-92 cells (B, C) were cocultured for 4 h with target cells at the indicated Effector:Target ratios. Cells were harvested and dead CTV⁺ target cells were quantified after PI labeling. (D) PBMCs were preconditioned overnight with the indicated Huh7 supernatant or control medium before introducing volume-to-volume K562NL target cells at the indicated ratios. After 4 h, NanoLuc release by target cell lysis was monitored. Means \pm SEM are shown for $n = 3$ (A, C), $n = 4$ (B), or $n = 6$ (D). p -values were obtained from two-way ANOVA analyses with Dunnett's post hoc test. * $p < 0.05$, ** $p < 0.01$

cells [8]. To further extend this observation, we compared the susceptibility of liver cancer cells expressing HK2 and/or GCK to cytolysis either by IL2-stimulated PBMCs which contain activated NK cells (Fig. 1A) or by the NK cell line NK-92 (Fig. 1B and C). Susceptibility to cytolysis by NK cells was similar between Huh7 cells transduced for GCK expression (Huh7-GCK⁺) and the parental Huh7 cells. In contrast, cells expressing only GCK after HK2 invalidation (Huh7-GCK⁺/HK2⁻) were much more susceptible to cytolysis than Huh7 cells (Fig. 1A and B). Although the percentage of target cell lysis was higher with NK-92 cells (Fig. 1B) than with PBMCs, which contain only 5 to 20% of NK cells (Fig. 1A), the greater susceptibility of Huh7-GCK⁺/HK2⁻ cells was observed in both cases. Similar results were obtained with the hepatoblastoma cell line Huh6 (Fig. 1C). Indeed, cells that were engineered by lentiviral transduction to knock down HK2 and express GCK (Huh6-GCK⁺/HK2⁻) (Supporting Information Fig. S1), showed greater susceptibility to cytolysis by NK cells than the parental Huh6 cells. In contrast, GCK transduction alone had no effect (Fig. 1C). We also analyzed the impact of soluble factors secreted by HCC cells on human NK-cell function. Since supernatants from HCC cell cultures did not interfere with the ability of PBMCs to kill K562, NK-sensitive target cells (Fig. 1D), we ruled out a role of soluble factors released by Huh7 cells in the inhibition of NK-cell function. These results suggest that HK2 expression confers to liver cancer cells a higher resistance to cytolysis by NK cells with a dominant effect over GCK expression.

HK2 binding at the mitochondria promotes Huh7 cell's resistance to cytolysis by NK cell

To further confirm the role of HK2 expression in the resistance of human liver tumor cells to cytolysis, Huh7-GCK⁺/HK2⁻ cells that are sensitive to NK cells, were transduced to re-express HK2 (Fig. 2A). Alternatively, and in order to test the role of HK2 binding to mitochondria in cellular resistance to cytolysis, we also re-expressed in these cells a mutant form of HK2 deleted of the N-terminal mitochondrial binding domain (HK2 Δ 10) [32]. After the selection of transduced cells with antibiotics, we obtained two new cell lines: Huh7-GCK⁺/HK2⁺ where full-length HK2 is re-expressed, and Huh7-GCK⁺/HK2 Δ 10⁺ that express the truncated HK2 (Fig. 2A and B). To validate the subcellular localization of HK2 vs. HK2 Δ 10, HK2 content in the mitochondrial fraction was analyzed. Results showed that HK2 Δ 10, like GCK, was much less associated with the mitochondrial fraction than full-length HK2 (Fig. 2B). This demonstrates that as expected, re-expressed HK2 binds to mitochondria whereas HK2 Δ 10 does not.

The re-expression of HK2 or HK2 Δ 10 in these cells resulted in increased glycolysis, as assessed by measuring the rate of acidification of the extracellular medium (glycolytic proton efflux rate) (Fig. 3A). Since hexokinase is a rate-limiting enzyme of the glycolysis, this indicates that both HK2 and HK2 Δ 10 are enzymatically functional. We then analyzed the mitochondrial respiration and as previously observed [8], the oxygen consumption rate was higher in Huh7-GCK⁺/HK2⁻ cells compared with parental Huh7 cells

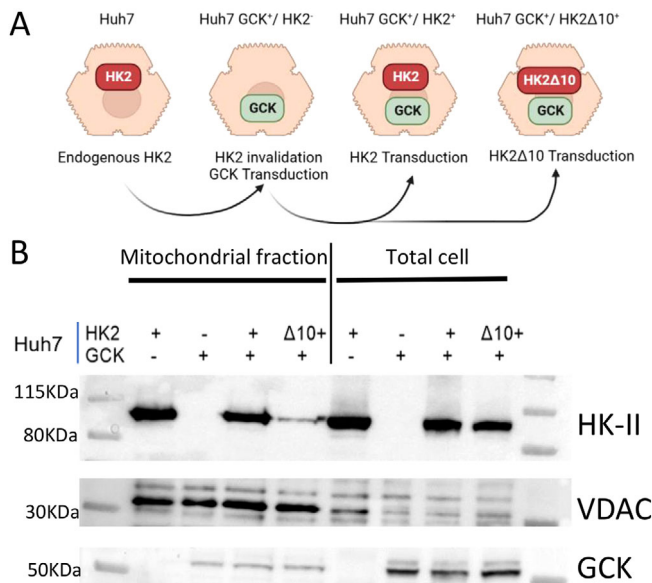


Figure 2. Engineering Huh7-derived cell lines, expressing metabolically active HK2 or HK2Δ10. The Huh7-GCK⁺/HK2⁻ cell line was engineered from Huh7 cells as previously described [8]. HK2 or HK2Δ10 were re-expressed in Huh7-GCK⁺/HK2⁻ cells by lentiviral transduction. (A) BioRender was used to illustrate cell line engineering. (B) GCK and HK2 expression and mitochondrial localization were compared for Huh7 (endogenous HK2), Huh7-GCK⁺/HK2⁻, Huh7-GCK⁺/HK2⁺, and Huh7-GCK⁺/HK2Δ10⁺ cell lines.

expressing HK2 (Fig. 3B and D). Interestingly, the re-expression of full-length HK2 but not HK2Δ10 in Huh7-GCK⁺/HK2⁻ cells resulted in a reduction of mitochondrial respiration, especially of the maximal respiration capacity of cells (Fig. 3D). In contrast, mitochondrial mass was unchanged (Fig. 3E), nor cell content in ATP synthase subunit ATP5B (Fig. 3F). Mitochondrial membrane potential was measured using TMRM fluorescent probe with CCCP treatment as negative control to measure basal labeling (Fig. 3G). There was no significant difference between cell lines, although the Huh7 parental cell line had slightly higher membrane potential. This indicates that mitochondrial HK2 binding does not significantly impact mitochondrial membrane polarization. Altogether, these results show that HK2 binding to mitochondria affects oxidative phosphorylation (OXPHOS) in Huh7 cells, which is in agreement with previous reports showing a similar effect in other cellular models [33]. These results also confirm the differential impact of HK2 and HK2Δ10 on mitochondria.

To analyze the role of HK2 and its localization in cellular susceptibility to cytolysis, we performed cytotoxicity assays with the different target cells derived from the parental Huh7 cell line: Huh7-GCK⁺, Huh7-GCK⁺/HK2⁻, Huh7-GCK⁺/HK2⁺, and Huh7-GCK⁺/HK2Δ10⁺. Cells were cocultured with NK-92 cells at an effector-to-target ratio of 10 and the number of dead target cells was determined by flow cytometry. As previously observed Huh7-GCK⁺/HK2⁻ cells were more sensitive to NK-induced cytolysis than Huh7 cells (Fig. 4A). Results showed that HK2 but not HK2Δ10 re-expression in Huh7-GCK⁺/HK2⁻ cells reduced the lysis of target cells (Fig. 4A). This demonstrates that HK2, through its binding to mitochondria, inhibits cytolysis by NK cells.

This could be attributed to differences in the activation of NK cells by the different target cell lines. Since IFN-γ is a validated marker of NK cell activation, we measured this cytokine in supernatants of NK cells after 4h of coculture with the different cell lines of interest. As expected, IFN-γ accumulation in culture supernatants is commensurate with the number of NK cells, but no differences were observed between the different target cell lines (Fig. 4B). These results indicate that Huh7 cells expressing GCK or HK2 have similar abilities to activate NK cells in vitro. Moreover, the reduced cytolysis of HK2-expressing cells was not correlated with the membrane expression of NK cell ligands such as ICAM-1, PVR (CD155), HLA-A,B,C, MIC-A/B, ULBP1, ULBP2/5/6 or ULBP3 (Supporting Information Figs. S2 and S3). When detected, the expression of these markers did not vary between the different target cell lines nor did they correlate with sensitivity to cytolysis by NK cells. Overall, this suggests that resistance to cytolysis provided by HK2 expression is linked to target cells' intracellular mechanisms and requires mitochondrial binding of HK2.

HK isoenzyme shift modulates caspase activity in Huh7 cells

Our results thus point toward differential sensitivity of Huh7-derived cell lines to NK-cell killing. NK cells induce target cell apoptosis by both the intrinsic pathway, involving cytochrome c release by mitochondria, and the extrinsic pathway, involving death receptor signaling by FAS and TRAIL receptors [34]. Both pathways initiate caspase-dependent apoptotic cell death. Since HK2 mitochondrial binding is associated with Huh7 cell's resistance to NK-cell cytotoxicity (Fig. 4A), we analyzed the effect of HK2 or HK2Δ10 expression on the activity of effector caspases 3 and 7. We found that the re-expression of HK2 but not HK2Δ10 into Huh7-GCK⁺/HK2⁻ cells reduced by 30% basal caspase 3/7 activity (Fig. 5A). As expected, caspase 3/7 activity was strongly induced by NK cell cytotoxicity, in all Huh7-derived target cells (Supporting Information Fig. S4). However, upon NK-cell activation, caspase 3/7 activity remained 30% lower in cells re-expressing HK2 but not in those expressing HK2Δ10 compared with the parental cell line (Fig. 5A). Therefore, HK2 expression and mitochondrial binding reduce effector caspase activity at the basal stage and this difference is maintained upon NK-cell-induced cell death.

HK isoenzyme shift modulates mitochondrial sensitivity to truncated BID

Since mitochondria play a major role in apoptosis and in the regulation of caspase 3/7 activation, we compared the sensitivity of the mitochondria isolated from the different Huh7 cell lines to BID (BH3-interacting domain death agonist) stimulation. Upon proteolysis by granzymes or caspase 8, truncated BID (tBID) can promote cytochrome c release from mitochondria, priming the assembly of the apoptosome. We thus treated the same quan-

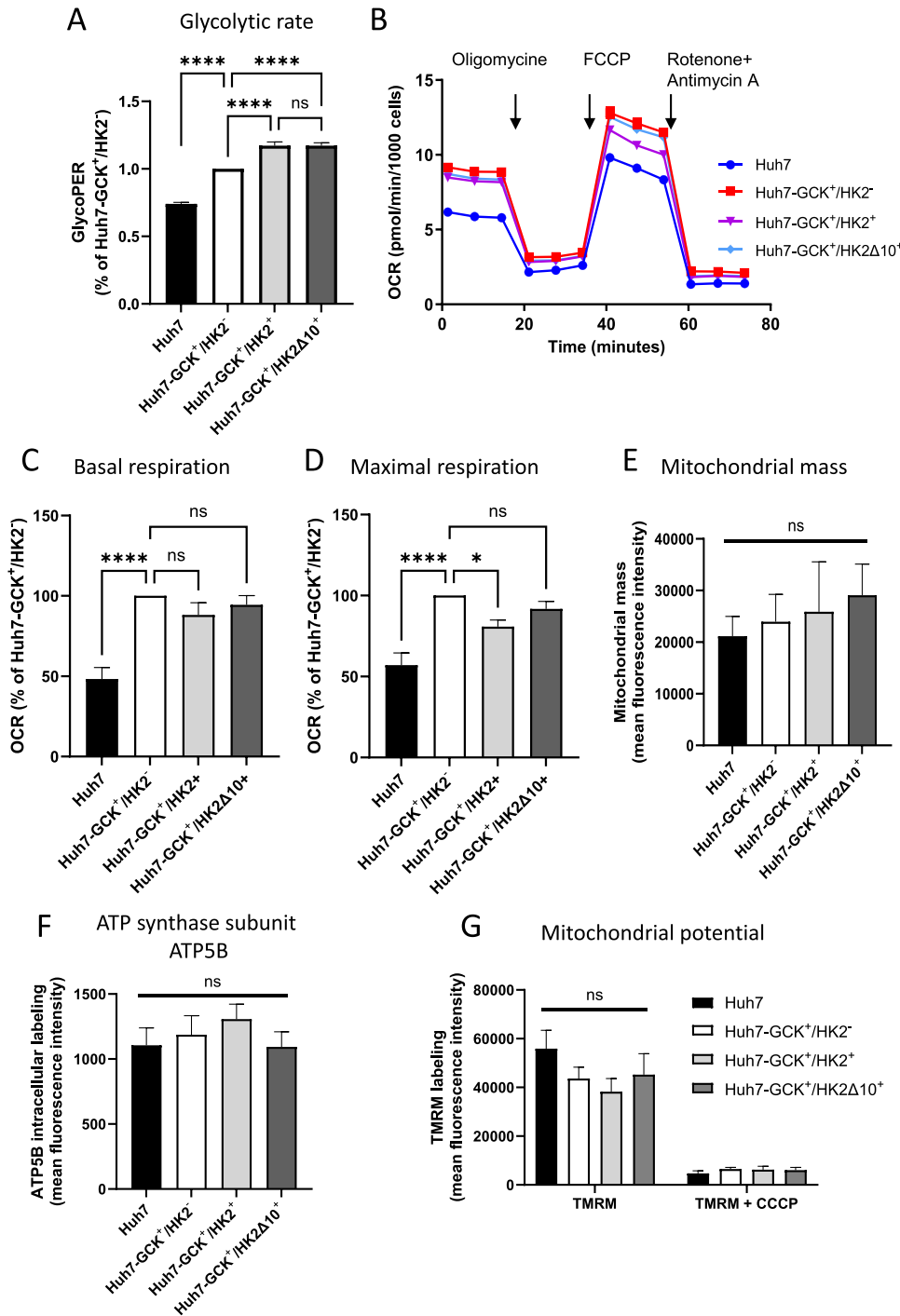


Figure 3. Impact of HK2 expression and mitochondrial binding on cell metabolic activity. (A) Basal glycolytic activity was measured with a XFe24 Seahorse analyzer in Huh7-GCK⁺/HK2⁻ re-expressing HK2 or HK2Δ10. (B) Oxygen consumption rate (OCR) was monitored with an XFe96 Seahorse analyzer using the Mito stress test to compare mitochondrial respiration of Huh7-derived cell lines, expressing HK2 or HK2Δ10 with or without GCK. (C, D) Impact of HK2 or HK2Δ10 re-expression in Huh7-GCK⁺/HK2⁻ cells on the basal (C) and maximal (D) respiration capacity of cells. (E) Mitochondrial mass analyzed by flow cytometry after MitoTracker Green labeling. (F) Intracellular content of mitochondrial ATP synthase subunit 5B monitored by flow cytometry. Mean fluorescence intensity was determined by subtracting the signal from the isotype control. (G) Mitochondrial membrane potential was analyzed using TMRM fluorescent probe labeling and flow cytometry. Cells were treated by CCCP to dissipate the transmembrane potential. Means ± SEM are shown and p values were determined using one-way ANOVA analyses with Holm-Šidák's post hoc test (n ≥ 3 independent experiments). *p < 0.05, ****p < 0.0001.

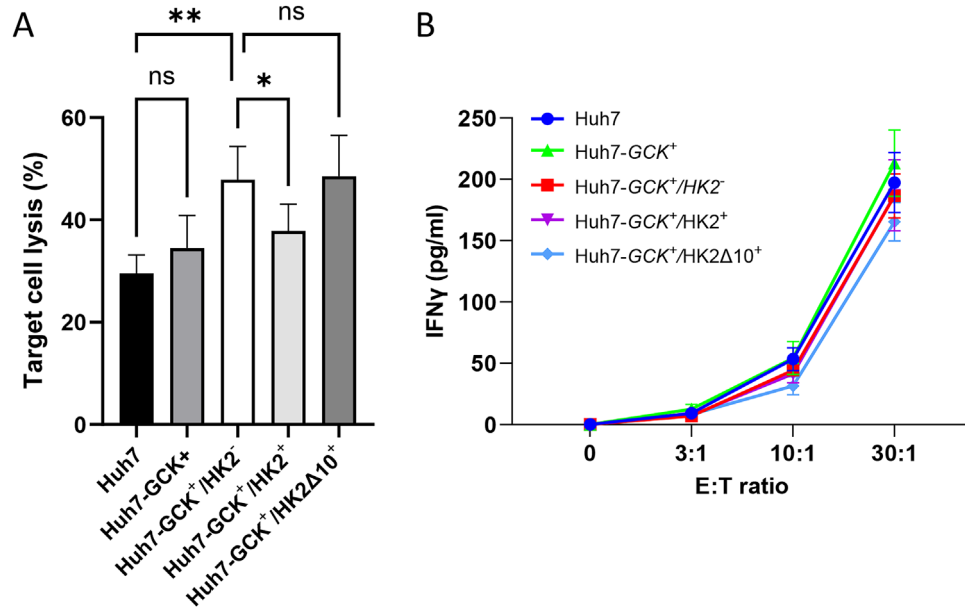


Figure 4. Mitochondrial binding of HK2 inhibits NK cell-mediated cytotoxicity of Huh7 cells. (A) Huh7-derived cell lines, expressing HK2 or HK2Δ10 with or without GCK were labelled with CTV and seeded. After 24 h, they were cocultured with NK-92 cells for 4 h at Effector:Target (E:T) ratio of 10. Target cell lysis was determined by the percentage of PI⁺ amongst CTV⁺ cells. (B) Supernatants were collected after 4 h coculture at E:T ratios from 3 to 30. IFN-γ was assayed by CBA. Means ± SEM are shown (n = 3), *p < 0.05, **p < 0.01, one-way ANOVA analyses with Tukey's post hoc test.

tivity of mitochondria isolated from the different Huh7 cell lines with increasing concentrations of tBID and cytochrome c release was quantified in mitochondria supernatants by automated capillary electrophoresis and immunodetection (Fig. 5B). Cytochrome c release was induced according to tBID concentration in an exponential manner. In order to compare the sensitivity to tBID of mitochondria from each cell line, we determined the EC₅₀ of tBID using nonlinear curve fitting (Fig. 5C). Variation of EC₅₀ according to HK2 or HK2Δ10 expression was analyzed compared with control Huh7-GCK⁺/HK2⁻ cell line (Fig. 5D). We found that HK2 expression but not HK2Δ10 increased by 2.5-fold the amount of tBID necessary to reach the EC₅₀ (Fig. 5D). This indicates that mitochondrial binding of HK2 protects mitochondria from tBID-induced cytochrome c release. This correlates with the increased resistance of HK2-expressing cells to NK-cell-induced cytotoxicity (Fig. 4A) and the decreased basal level of caspase activity (Fig. 5A) in these cells.

Discussion

Our results indicate that both an HCC cell line (Huh7) and a hepatoblastoma cell line (Huh6) were more resistant to NK-cell cytotoxicity when they expressed the tumor isoenzyme HK2 rather than the liver isoenzyme GCK. It was found that HK2 expression correlates with the progression of many cancers [35] and is associated with a higher risk of liver cancer development [25]. Moreover, previous results, including ours, indicated that high HK2 expression is correlated with poor survival of HCC patients [8, 36]. In Huh7 cells, DeWaal et al. [24] demonstrated that the depletion of HK2 suppressed glycolytic metabolism and

promoted OXPHOS. Consistently, we showed that expression of HK2, instead of GCK, increased lactate production and inhibited mitochondrial respiration in Huh7 cells [8]. This work shows that HK2 tethering to mitochondria reduces OXPHOS activity in Huh7 cells, without affecting mitochondrial mass and polarization (Fig. 3). In other cancer cells, HK2 expression and binding to the outer mitochondrial membrane protein VDAC was involved in this metabolic switch known as the “Warburg effect” [37]. Hence, both increased expression and mitochondrial binding of HK2 are thought to modulate cell metabolism. HK2 binding to mitochondria can be modulated by the concentration of metabolites such as G6P which promotes HK2 detachment. G6P also inhibits HK2 binding to mTORC1 via the FDIDI motif located in the first HK domain of HK2 [28], therefore regulating energy production [27]. Upon starvation, the absence of G6P allows HK2 interaction with mTORC1, promoting autophagy and energy conservation [28]. Since G6P is fueling not only the glycolysis but also the pentose phosphate pathway and glycogenesis, the modulation of these metabolic pathways could impact HK2 localization in tumor cells and therefore also modify the sensitivity of cancer cells to NK cytotoxicity.

It has been shown that the important glycolytic activity of tumor cells results in some alterations in the tumor microenvironment. In particular, tumor-derived lactate secreted in the extracellular space can affect the survival and function of NK cells, reducing the cytotoxic activity of NK cells with impaired IFN-γ secretion [38]. In our in vitro model, supernatants from Huh7 cells were unable to inhibit the cytotoxic activity of NK cells toward highly sensitive targets (Fig. 1D). Furthermore, secreted levels of IFN-γ were similar in co-cultures of NK cells with the different Huh7 cell lines, thus demonstrating that NK activation was com-

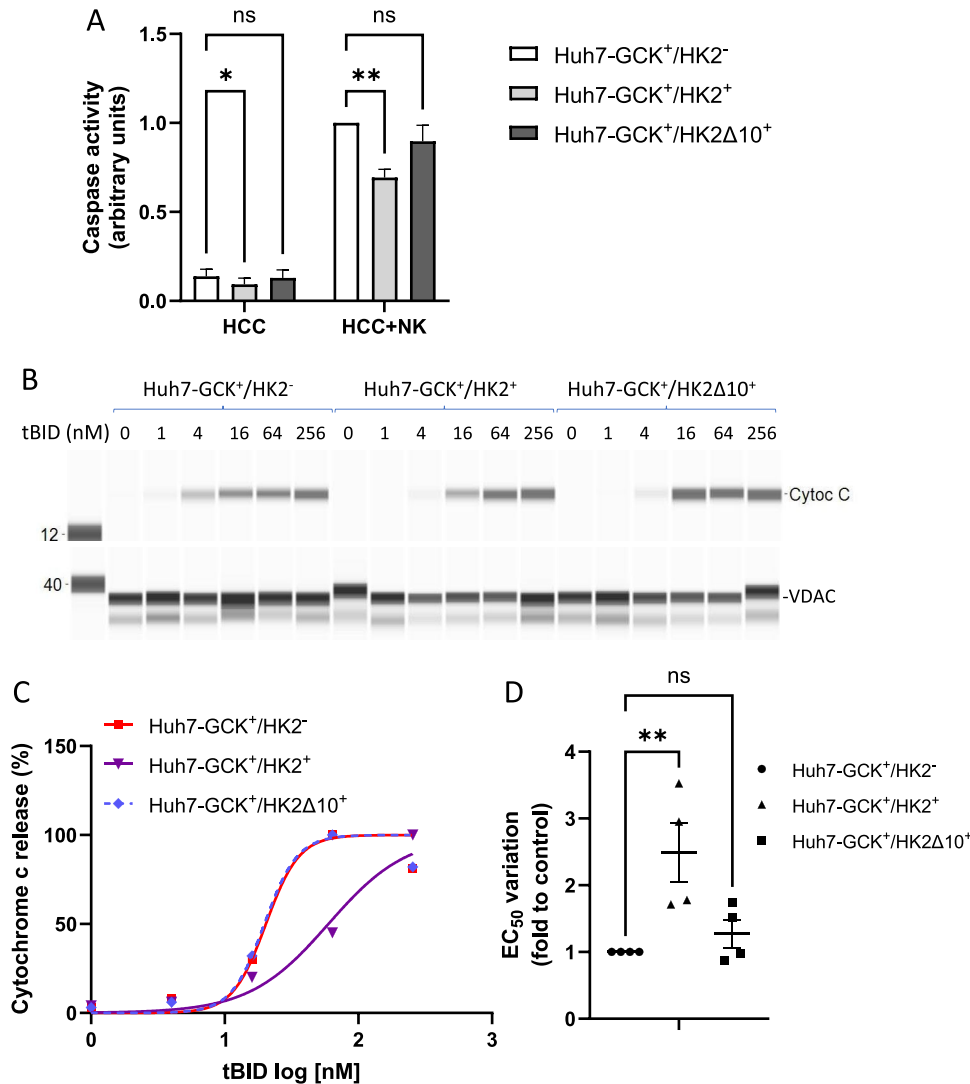


Figure 5. HK2 binding determines mitochondria sensitivity to cell death signals. (A) HK2, but not HK2Δ10 re-expression in Huh7-GCK⁺/HK2⁻ cells, modulates effector caspase 3/7 activity at basal stage (HCC) and upon activation by NK cells (HCC+NK). Caspase activity was reported to that of Huh7-GCK⁺/HK2⁻ HCC cells induced by NK cells. Means ± SEM (n = 7) are shown and p values were determined using two-way ANOVA. *p < 0.05, **p < 0.01 (B–D) tBID-induced cytochrome (Cytoc) c release by mitochondria isolated from Huh7-GCK⁺/HK2⁻, Huh7-GCK⁺/HK2⁺, or Huh7-GCK⁺/HK2Δ10⁺. Representative experiment showing Cytoc c expression in the supernatant of mitochondria and VDAC expression in mitochondria lysates. Analysis was performed by automated capillary electrophoresis and immunodetection (B). Molecular weight markers (kDa) are indicated in the first lane left. Nonlinear curve fitting of Cytoc c release as a function of tBID concentration determining the EC₅₀, for a representative experiment (C). EC₅₀ variation in fold to control, according to HK2 or HK2Δ10 re-expression in Huh7-GCK⁺/HK2⁻ cells (D). Means ± SEM are shown for four independent experiments. **p < 0.01, one-way ANOVA.

parable (Fig. 4B). We observed an increased glycolytic activity upon expression of both HK2 and HK2Δ10 in Huh7-GCK⁺/HK2⁻ (Fig. 3A) that was decoupled with the modulation of their killing by NK cells (Fig. 4A), indicating that enhanced glycolysis does not induce NK cell resistance. Our results rather indicate that HK2 mitochondrial localization contributes to liver cancer cells resistance to NK-cell-mediated cytotoxicity, probably by interfering with cytochrome c release by mitochondria and cell death triggering (Fig. 5).

HK2 binding to mitochondria is mediated by VDAC, an integral membrane protein in the outer mitochondrial membrane, located at contact sites between outer and inner mitochondrial mem-

branes. This channel contributes to exchanges of NAD⁺/NADH, ADP/ATP, succinate, citrate, and ions between the cytosol and mitochondria. VDAC is also involved in the release of cytochrome c from the mitochondrial intermembrane space, a process that may be controlled by its interaction with pro or anti-apoptotic proteins of the BCL-2 family [39]. In acellular systems, it was shown that pro-apoptotic proteins BAX, BAK, and BIM induce the formation of a large pore formed by their interaction with VDAC [40]. During chronic liver damage, it is known that apoptosis is regulated by pro-apoptotic BCL-2 proteins, BAX and BAK. These factors permeabilize the outer mitochondrial membrane and release intermembrane space proteins, such as cytochrome c,

into the cytoplasm. The release of cytochrome c then triggers the assembly of the apoptosome which participates in the activation of caspases, finally resulting in cell death. Inhibition of proapoptotic proteins or caspases and activation of pro-survival genes contribute to liver cancer development and progression. Therefore, HK2 expression and its association with the mitochondrial membrane of hepatocytic cells could modulate VDAC activity and consequently apoptosis regulation, explaining the higher resistance of Huh7 cells expressing HK2 to NK-cytotoxicity. Indeed, in HCC there is an imbalance between the pro- and anti-apoptotic of BCL-2 family members, and defects in apoptosis signaling contribute to the chemotherapy resistance [41].

Interestingly, several mechanisms have been attributed to HK2 for its protection against apoptosis although, the molecular basis of this apoptosis inhibition remains unresolved [42]. Previous reports showed that HK1 and HK2 proteins could interfere with intramembranous oligomerization of BAX, inhibiting the formation of pores [43]. In contrast to other studies where HK2 deletion results in drastic restriction of glycolytic activity, we analyzed the role of HK2 in cells where glycolysis remained functional because GCK expression was restored before HK2 deletion [8]. Our metabolic measurements showed that the glycolytic activity remained high (Fig. 3A) and no significant difference was observed in the basal cell death rate regardless of the type of HK expressed in hepatocytes (Fig. 1). Previous studies have also shown that BID activation is crucial in hepatocyte apoptosis induced by FAS/TNF-R1 signals [44, 45]. Hepatocytes require a BID-dependent mitochondrial amplification loop that releases cytochrome c, oligomerizing APAF1, and caspase-9 to activate sufficient effector caspases to execute apoptosis [46]. A crosstalk between extrinsic death signals (FAS L/FAS receptor signaling) and the granzyme B-induced apoptosis pathway results from common proteolysis of BID protein, by either caspase 8 or granzyme B, into its active form tBID [34]. It was previously reported that HK1 could bind and inhibit tBID, accelerating its retrotranslocation from mitochondria to cytosol [43]. HK inhibition of cytochrome c release was thought to be specific to death-receptor-induced apoptosis [43]. In contrast, our results indicate that HK2 binding to the mitochondria directly increases the resistance of mitochondria to cytochrome c release induced by tBID (Fig. 5B–D). Therefore, more activated BID is probably needed to launch mitochondrial apoptosis in HCC cells expressing HK2, explaining their reduced effector caspase activity (Fig. 5A). This mechanism establishes a direct connection between HK2 expression and the resistance of liver cancer cells to cell death triggered by NK cells, extending previous observation of HK-dependent resistance to death receptor ligands [43].

These findings indicate that the switch of HK from GCK to HK2, especially during HCC development, not only rewires cell metabolism to support proliferation but also promotes tumor cell resistance to NK cell-induced cytotoxicity. This reinforces interest in HK2 as a potentially important molecular target for anti-tumoral therapy. Glycolytic inhibitors like 2-deoxyglucose or 3-bromopyruvate targeting the activity of this enzyme have proved difficult to use in clinics. Novel HK2 enzyme inhibitors are being

developed, inducing apoptosis of tumor cells and inhibiting tumor growth in xenograft mouse models [47]. However, the selectivity to HK2 vs HK1, HK3, or GCK is very difficult to achieve due to similarities in the enzyme function. Developing pharmacological agents targeting HK2-VDAC interaction rather than the HK2 glycolytic activity could be a valuable antitumoral strategy to promote innate immunity and favor NK cell-induced cytotoxicity without affecting cells expressing other HK isoenzymes.

Material and methods

HK2 and HK2Δ10 cloning and production of lentiviral vectors

The human HK2 ORF cloned in the pDONR223 plasmid was obtained from the ORFeome library [48]. The ORF corresponding to HK2 deleted of the first 10 amino acids (HK2Δ10) was generated by PCR using the following primers: HK2Δ10_forward_GGGGACAACCTTTGTACAAAAGTTGGCATGTT-CACGGAGCTCAACCATG and HK2_Rreverse_GGGGACAACCTTTGTACAA-GAAAGTTGGTTATCGCTGTCCAGCCTCACGGA, and cloned into pDONR223 by BP recombination (Gateway system; Thermo Fisher) and sequenced. HK2 and HK2Δ10 ORFs were then transferred by LR recombination (Gateway system) into the pLenti-PGK-Neo-DEST to obtain pLenti-PGK-HK2 and pLenti-PGK-HK2Δ10 plasmids. pLenti-PGK-Neo-DEST (w531-1) was a gift from Eric Campeau & Paul Kaufman (Addgene plasmid # 19067; <https://n2t.net/addgene:19067>; RRID:Addgene_19067).

To generate lentiviral particles with the constructs described above, 4×10^6 HEK-293T cells were seeded in 10 cm Petri dishes. The day after, cells were co-transfected using the Calcium-Phosphate method with packaging (PAX2), envelope (pCMV-VSV-G), and pLenti-PGK-HK2 or pLenti-PGK-HK2Δ10 plasmids. Cells were incubated at 37°C for 6 h, and the transfection medium was replaced with fresh OPTIMEM (Life Technologies) supplemented with 1% penicillin/streptomycin (P/S) and HEPES buffer. 36 h posttransfection, cell culture supernatants containing lentiviral particles were collected, filtered on 0.45 μm pore-size membranes, and stored at –80°C.

shHK2 cloning and production of lentiviral vectors

The pLKO.1-shHK2 vector was obtained by ligation of two annealed oligos (forward_CCGGCCAGAAGACATTAGAGCATCTCTCGAGAGATGCTCTAATGTCTTCTGGTTTTTT and reverse_AATTAAAAAACCAGAAGACATTAGAGCATCTCTCGAGAGATGCTCTAATGTCTTCTGG) into pLKO.1 hygro vector (Addgene #24150). To generate lentiviral particles encoding the shRNA against HK2 (shHK2), 2.5 million HEK-293T cells were seeded. The day after, cells were co-transfected using jetPEI transfection reagent (Polyplus transfection) with packaging pCMV-dR8.91, pLKO.1-shHK2, and envelope (pCMV-VSV-G) plasmids. After 6 h of incubation at

37°C, the culture medium was replaced. At 36 h posttransfection, the cell culture supernatant containing lentiviral particles was collected, filtered on 0.45 µm pore-size membrane, and stored at -80°C.

Cell lines

Huh7 cells were transduced for GCK expression as previously described [8]. The Huh7-GCK⁺ cells were then cultured for 7 days with puromycin (1 µg/mL) before amplification. HK2 knock-out was achieved using the CRISPR/Cas9 system as previously described to obtain Huh7-GCK⁺/HK2⁻ cells [8]. To express HK2 or HK2Δ10, Huh7-GCK⁺/HK2⁻ cells were transduced with lentiviral particles containing either HK2 or HK2Δ10 and selected with neomycin for at least 2 weeks. Huh6-GCK⁺ cells were obtained by GCK transduction of Huh6 cells using the same method. Huh6-GCK⁺/HK2⁻ were obtained after HK2 knock-down by transduction with lentiviruses expressing shHK2 and selection with hygromycin (200 µg/mL). HK2 and GCK expression in cell lines was monitored by Western blotting (Supporting Information Fig. S1).

Western blotting

Cell lysates from 10⁶ cells were prepared in lysis buffer (20 mM Tris-HCl pH 7.4, 1 mM EDTA, 180 mM NaCl, 0.5% NP40 with 1% protease inhibitor cocktail (Sigma-Aldrich, P8340)). After the elimination of insoluble material, proteins were quantified, separated by SDS-PAGE, and analyzed by western-blot on nitrocellulose membrane. After saturation of the nitrocellulose membrane in PBS-0.1% Tween 20 supplemented with 5% (w/v) non-fat-milk powder, blots were incubated 1 h at room temperature with primary antibody in PBS-0.1% Tween 20 (1:1000 dilution), mouse monoclonal antibody against human GCK (clone G-6, Santa Cruz Biotechnology), rabbit monoclonal antibody against human HK2 (Clone C64G5, Cell Signaling Technology). Incubation with a secondary antibody was performed after washing for 1 h at room temperature. HRP-labelled anti-rabbit (Sigma-Aldrich, A0545) or anti-mouse (Jackson ImmunoResearch Laboratories) antibodies were diluted 10 000 folds and detected by enhanced chemiluminescence reagents according to the manufacturer's instructions (SuperSignal Chemiluminescent Substrate, Thermo Fisher Scientific).

Cell culture

All Huh7 and Huh6 cell lines were cultured in DMEM with 4.5 g/L D-glucose without phenol red supplemented with 10% FCS (BioSera), 2 mM L-glutamine, 1% P/S, and 1 mM pyruvate. All reagents were from Life Technologies except FCS.

Natural Killer NK-92 cells were grown in RPMI 1640 Medium with Glutamax supplemented with 10% FCS (BioSera), 1% P/S, 1 mM pyruvate, 10 mM HEPES buffer, 50 µM β-mercaptoethanol,

and 100 IU/mL of human IL-2 (R&D Systems) to promote cellular proliferation. All cell lines were incubated at 37°C with 5% CO₂. Reagents were from Life Technologies unless specified.

The K562 cell line expressing the luciferase NanoLuc (K562NL) was previously described [49] and cells were grown in RPMI 1640 Medium with Glutamax supplemented with 10% FCS (BioSera) and 1% P/S.

Blood cells preparation

Human blood was provided by the Etablissement Français du Sang and informed consent was obtained from donors. No individual participant information was obtained or included. PBMCs were isolated by standard density gradient centrifugation on the Ficoll/Diatrizoate separation medium (*d* = 1.077, Eurobio Scientific). NK cells in PBMCs were stimulated overnight with IL-2 (200 IU/mL; R&D Systems) in RPMI 1640 Glutamax Medium with 10% FCS (Corning) and 40 µg/mL gentamycin.

Cytotoxicity assay

Target cells were labeled with Cell Trace Violet (CTV, Life Technologies) and seeded at 1 × 10⁵ cells per well in a 24-well plate in DMEM (Gibco) with 10% FCS, 2 mM L-glutamine, 1% P/S, and 1 mM pyruvate. After 24 h, prestimulated PBMCs or NK-92 effector cells were added to target cells at the indicated effector-to-target cell ratios. The cytotoxicity assay was performed for 4 h at 37°C, under 5% CO₂. Supernatants were collected and cells were harvested after trypsinization. Target hepatoma cell death was monitored by propidium iodide labeling and flow cytometry analysis of CTV-labelled hepatocytes on a FACS Canto II device (BD Biosciences). IFN-γ was quantified in clarified supernatants of cytotoxicity assays by Cytometric Bead Array (CBA, BD Biosciences, 558269).

PBMCs were preconditioned overnight with a 24 h-supernatant of one of the HCC target cells or with a control medium and mixed volume to volume with K562NL sensitive target cells to obtain the indicated effector-to-target cell ratios. NanoLuc release induced by target cell lysis was measured in the co-culture supernatant as previously described [49].

Metabolic activity monitoring with Seahorse XFe analyzer

Twenty-four hours prior to the assay, 5 × 10⁴ cells/well or 1.6 × 10⁴ cells/well cells were seeded in 24- or 96-wells Seahorse XF cell culture microplates (Agilent), respectively, pre-coated with 0.01% poly-L-Lysine (Sigma-Aldrich) and incubated at 37°C with 5% CO₂ in DMEM supplemented with 10% FCS (BioSera), 1 mM pyruvate, 2 mM L-glutamine, 1% P/S. One hour prior to the assay, cells were washed with Seahorse assay medium (XF DMEM pH7.4 + 10 mM Glucose, 2 mM Glutamine, and 1 mM sodium pyruvate) and incubated at 37°C in a non-CO₂ incubator. Metabolic activi-

ties were monitored with the Seahorse XFe24 Analyzer or XFe96 Analyzer (Agilent) in 500 or 180 μ L of Seahorse assay medium, respectively. Glycolytic activity was measured using the Glycolytic Rate Assay (Agilent). Glycolytic proton efflux rate was calculated by subtraction of mitochondrial-associated acidification to total PER. The oxygen consumption rate was measured using the Seahorse XF Cell Mito Stress Test (Agilent). The number of cells was determined at the end of each run after Hoechst staining and cell counting using a Biotek Cytation 1 imaging reader (Agilent).

Flow cytometry

Cells were detached with 1X citrate buffer (135 mM potassium chloride, 15 mM sodium citrate in water) for 10 min at 37°C, washed, and resuspended in a solution containing the antibodies of interest diluted in FACS buffer (PBS with 0.1% BSA and 0.05% sodium azide). The cells were incubated for 30 min at 4°C with directly coupled fluorescent antibodies and washed twice in FACS buffer before being analyzed on the FACS Canto II cytometer (BD Biosciences). Following mouse antibodies were used: IgG2a-PE (isotype control, Beckman Coulter, A09142), IgG1-FITC (isotype control, Beckman Coulter, A07795), monoclonal REA control antibody-APC (universal isotype control, Miltenyi Biotec), anti-human PVR-PE (BD Biosciences, 566718), anti-human ICAM-1-FITC (Beckman Coulter, IMO726U), anti-human MIC-A/B-PE (BD Biosciences, 558352), anti-human HLA-A,B,C-FITC (BD Biosciences, 555552), anti-human ULBP1-APC, ULBP3-APC, ULBP2/5/6-APC (R&D Systems, FAB1380A, FAB1517A, FAB1298A). Cell content in the ATP synthase subunit (ATP5B) was measured by intracellular staining. Briefly, cell suspensions were fixed and permeabilized with Cytofix/Cytoperm reagents (BD Biosciences). Two-step-labeling was performed using mouse anti-ATP5B antibody (Origene, TA500851S) or mouse IgG1 (eBioscience, 16-4714-82) as isotype control and Alexa Fluor 488-goat anti-mouse secondary antibody. Cells were washed in Perm/Wash buffer after each step and before analyses using a FACS LRSII cytometer (BD Biosciences). MitoTracker Green FM (Invitrogen, M7514) and TMRM (Invitrogen, M20036) probes were used to monitor mitochondrial total mass and mitochondrial membrane potential, respectively. Monolayer cells were incubated for 30 min at 37°C and 5% CO₂ with these fluorescent probes before being detached and analyzed on the FACS Canto II cytometer (BD Biosciences) for MitoTracker and FACS LRSII cytometer (BD Biosciences) for TMRM. Before TMRM labeling, cells were treated with the depolarizing agent CCCP (50 μ M) or DMSO as solvent control for 5 min at 37°C. Flow cytometry results were acquired and analyzed in agreement with published guidelines [50], using FlowJo v10 software, after gating on all cells using morphological parameters.

Caspase activity

Twenty-four hours prior to the assay, 12×10^3 target cells per well were seeded in a 96-well plate. When indicated, NK-92

cells were added to the targets at the indicated effector-to-target cell ratios. After 1 h incubation at 37°C under 5% CO₂, caspase 3/7 activity was measured using Caspase-Glo 3/7 Assay Systems (Promega, G8090). Caspase activity was normalized by cell count after Hoechst staining and cell counting using a Biotek Cytation 1 imaging reader (Agilent) with ImageJ software processing.

Mitochondria preparation

One million cells were seeded in a 10 cm Petri dish with 10 ml of supplemented DMEM medium (see above). After 48 to 72 h of culture, cells were washed once with PBS and once with cold mannitol buffer (mannitol 210 mM, HEPES 10 mM pH 7.4, sucrose 70 mM, EDTA 1 mM). Cells were harvested by scraping in 2 mL of mannitol buffer supplemented with a protease inhibitor cocktail (Sigma-Aldrich, P8340). Cells from five dishes were pooled. After centrifugation at 1000 g for 5 min at 4°C, cells were resuspended in 1 mL of mannitol buffer with a protease inhibitor cocktail and transferred to the Dounce homogenizer to prepare cell lysates. After 25 up-and-down strokes, the homogenate was centrifuged as above to remove cellular debris. The supernatant containing the mitochondria was centrifuged at 10 000 g for 10 min at 4°C, and the pellet containing mitochondria was resuspended in 100 μ L of KCl buffer (KCl 125 mM, EGTA 0.5 mM, succinate 5 mM, HEPES-KOH 10 mM pH 7.4, MgCl₂ 4 mM, Na₂HPO₄ 5 mM) supplemented with protease inhibitors. Mitochondria were quantified by protein assay using the Bradford method against a BSA standard curve. The suspension of mitochondria was adjusted to 1 mg of protein/mL.

tBID-induced cytochrome c release

Mitochondria from each cell line (25 μ g/test) were treated with 5 μ L recombinant tBID protein (R&D Systems, 882-B8) to achieve final concentration of 256, 64, 16, 4, 1, or 0 nM. After 30 min incubation at 30°C in a water bath, mitochondria were centrifuged at 4°C for 10 min at 13 000 rpm. The supernatants, containing released cytochrome c, were collected and stored, along with the mitochondrial pellets, at -80°C before performing the protein analysis.

Automated western immunoblotting

Mitochondria pellets were lysed for 1 h at 4°C in 20 μ L CHAPS buffer 2% containing 50 U/mL benzonase and 1X protease inhibitor cocktail. Mitochondria lysates were diluted twice in Laemmli-TCEP 1X (Bio-Rad, 1610747 Laemmli 4X; ThermoFisher, T2556 TCEP). Mitochondria supernatants and diluted lysates were denatured with Fluorescent 5X Master mix (ProteinSimple) for 5 min at 95°C. Protein extracts were analyzed for cytochrome c and VDAC content with the Jess Simple Western System from Bio-Techne (12-230 kDa Fluorescence Separation Module, SM-FL001; EZ Standard Pack 1; PS-ST01EZ). Cytochrome c was detected

with anti-cytochrome c (Cell Signaling Technology, 4272) and HRP-coupled anti-rabbit antibody (ProteinSimple). VDAC was detected with anti-VDAC (Millipore, MABN504) and HRP-coupled anti-mouse antibody (ProteinSimple). Digital images of chemiluminescence were analyzed using Compass Simple Western software (version 4.1.0; ProteinSimple) to determine signal intensities. Cytochrome c release was normalized to total VDAC protein content in mitochondria pellets.

Statistics and reproducibility

All statistical analyses were performed with GraphPad Prism. Details of statistical analyses can be found in figure legends. Statistical analyses were performed on experiments reproduced at least 3 times independently. The mean \pm SEM is displayed and the exact sample size (n) is given in the legend of each figure. The confidence interval was set to 95% in all statistical tests.

Acknowledgements: The authors acknowledge the contribution of the Etablissement Français du Sang Auvergne - Rhône-Alpes and SFR Biosciences (UMS3444/CNRS, US8/Inserm, ENS de Lyon, UCBL) facilities: ANIRA-ImmOs Phenotyping for Real Time Metabolism Assays, ANIRA-Cytometry and Protein Science Facility for Automated Western Immunoblotting. We thank Julie Carron and Laetitia Voto for their technical assistance.

This research was funded by the Fondation pour la Recherche Médicale (FRM), grant number DEQ20160334893 to V.L. and by the Agence Nationale de Recherches sur le SIDA et les hépatites virales (ANRS), grant number ECTZ244976 to O.D.

Conflict of interest: The authors declare no financial or commercial conflict of interest.

Data availability statement: The data that support the findings of this study are available from the corresponding author upon reasonable request.

Peer review: The peer review history for this article is available at <https://publons.com/publon/10.1002/eji.202350954>

References

- Rumgay, H., Arnold, M., Ferlay, J., Lesi, O., Cabaasag, C. J., Vignat, J., Laveranne, M. et al., Global burden of primary liver cancer in 2020 and predictions to 2040. *J. Hepatol.* 2022. 77: 1598–1606.
- Chuang, W. L., Liu, H. W. and Chang, W. Y., Natural killer cell activity in patients with hepatocellular carcinoma relative to early development and tumor invasion. *Cancer* 1990. 65: 926–930.
- Jinushi, M., Takehara, T., Tatsumi, T., Hiramatsu, N., Sakamori, R., Yamaguchi, S. and Hayashi, N., Impairment of natural killer cell and dendritic cell functions by the soluble form of MHC class I-related chain A in advanced human hepatocellular carcinomas. *J. Hepatol.* 2005. 43: 1013–1020.
- Heinrich, B., Gertz, E. M., Schäffer, A. A., Craig, A., Ruf, B., Subramanyam, V., McVey, J. C. et al., The tumour microenvironment shapes innate lymphoid cells in patients with hepatocellular carcinoma. *Gut* 2021. 71: 1161–1175.
- Hack, S. P., Spahn, J., Chen, M., Cheng, A.-L., Kaseb, A., Kudo, M., Lee, H. C. et al., IMbrave 050: a Phase III trial of atezolizumab plus bevacizumab in high-risk hepatocellular carcinoma after curative resection or ablation. *Future Oncol.* 2020. 16: 975–989.
- Chew, V., Chen, J., Lee, D., Loh, E., Lee, J., Lim, K. H., Weber, A. et al., Chemokine-driven lymphocyte infiltration: an early intratumoural event determining long-term survival in resectable hepatocellular carcinoma. *Gut* 2012. 61: 427–438.
- Liu, P., Chen, L. and Zhang, H., Natural Killer Cells in Liver Disease and Hepatocellular Carcinoma and the NK Cell-Based Immunotherapy. *J. Immunol. Res.* 2018. 2018: 1206737.
- Perrin-Cocon, L., Vidalain, P.-O., Jacquemin, C., Aublin-Gex, A., Olmstead, K., Panthu, B., Rautureau, G. J. P. et al., A hexokinase isoenzyme switch in human liver cancer cells promotes lipogenesis and enhances innate immunity. *Commun. Biol.* 2021, 4: 217.
- Armeanu, S., Bitzer, M., Lauer, U. M., Venturelli, S., Pathil, A., Krusch, M., Kaiser, S. et al., Natural killer cell-mediated lysis of hepatoma cells via specific induction of NKG2D ligands by the histone deacetylase inhibitor sodium valproate. *Cancer Res.* 2005. 65: 6321–6329.
- Sun, X., Sui, Q., Zhang, C., Tian, Z. and Zhang, J., Targeting blockage of STAT3 in hepatocellular carcinoma cells augments NK cell functions via reverse hepatocellular carcinoma-induced immune suppression. *Mol. Cancer Ther.* 2013. 12: 2885–2896.
- Cadoux, M., Caruso, S., Pham, S., Gougelet, A., Pophillat, C., Riou, R., Loesch, R. et al., Expression of NKG2D ligands is downregulated by β -catenin signalling and associates with HCC aggressiveness. *J. Hepatol.* 2021. 74: 1386–1397.
- Bryceson, Y. T., March, M. E., Ljunggren, H.-G. and Long, E. O., Activation, coactivation, and costimulation of resting human natural killer cells. *Immunol. Rev.* 2006. 214: 73–91.
- Balzasch, B. M. and Cerwenka, A., Microenvironmental signals shaping NK-cell reactivity in cancer. *Eur. J. Immunol.* 2023. 0: 2250103.
- Raulet, D. H., Gasser, S., Gowen, B. G., Deng, W. and Jung, H., Regulation of ligands for the NKG2D activating receptor. *Annu. Rev. Immunol.* 2013. 31: 413–441.
- Diefenbach, A., Jensen, E. R., Jamieson, A. M. and Raulet, D. H., Rae1 and H60 ligands of the NKG2D receptor stimulate tumour immunity. *Nature* 2001. 413: 165–171.
- Bryceson, Y. T., March, M. E., Barber, D. F., Ljunggren, H.-G. and Long, E. O., Cytolytic granule polarization and degranulation controlled by different receptors in resting NK cells. *J. Exp. Med.* 2005. 202: 1001–1012.
- Urlaub, D., Höfer, K., Müller, M.-L. and Watzl, C., LFA-1 activation in NK cells and their subsets: influence of receptors, maturation, and cytokine stimulation. *J. Immunol.* 2017. 198: 1944–1951.
- Martinet, L. and Smyth, M. J., Balancing natural killer cell activation through paired receptors. *Nat. Rev. Immunol.* 2015. 15: 243–254.
- Poznanski, S. M., Singh, K., Ritchie, T. M., Aguiar, J. A., Fan, I. Y., Portillo, A. L., Rojas, E. A. et al., Metabolic flexibility determines human NK cell functional fate in the tumor microenvironment. *Cell Metab.* 2021. 33: 1205–1220.e5.
- Husain, Z., Huang, Y., Seth, P. and Sukhatme, V. P., Tumor-derived lactate modifies antitumor immune response: effect on myeloid-derived suppressor cells and nk cells. *J. Immunol.* 2013. 191: 1486–1495.

- 21 Marçais, A., Cherfils-Vicini, J., Viant, C., Degouve, S., Viel, S., Fenis, A., Rabilloud, J. et al., The metabolic checkpoint kinase mTOR is essential for IL-15 signaling during the development and activation of NK cells. *Nat. Immunol.* 2014. 15: 749–757.
- 22 Perrin-Cocon, L., Aublin-Gex, A., Diaz, O., Ramiere, C., Peri, F., Andre, P. and Lotteau, V., Toll-like receptor 4-induced glycolytic burst in human monocyte-derived dendritic cells results from p38-dependent stabilization of HIF-1 α and increased hexokinase II expression. *J. Immunol.* 2018. 201: 1510–1521.
- 23 Guzman, G., Chennuri, R., Chan, A., Rea, B., Quintana, A., Patel, R., Xu, P.-Z. et al., Evidence for heightened hexokinase II immunorexpression in hepatocyte dysplasia and hepatocellular carcinoma. *Dig. Dis. Sci.* 2015. 60: 420–426.
- 24 DeWaal, D., Nogueira, V., Terry, A. R., Patra, K. C., Jeon, S. M., Guzman, G., Au, J. et al., Hexokinase-2 depletion inhibits glycolysis and induces oxidative phosphorylation in hepatocellular carcinoma and sensitizes to metformin. *Nat. Commun.* 2018. 9: 446.
- 25 Lee, N. C. W., Carella, M. A., Papa, S. and Bubici, C., High expression of glycolytic genes in cirrhosis correlates with the risk of developing liver cancer. *Front. Cell Dev. Biol.* 2018; 6: 138.
- 26 Wolf, A. J., Reyes, C. N., Liang, W., Becker, C., Shimada, K., Wheeler, M. L., Cho, H. C. et al., Hexokinase is an innate immune receptor for the detection of bacterial peptidoglycan. *Cell* 2016. 166: 624–636.
- 27 Tan, V. P. and Miyamoto, S., HK2/hexokinase-II integrates glycolysis and autophagy to confer cellular protection. *Autophagy* 2015. 11: 963–964.
- 28 Roberts, D. J., Tan-Sah, V. P., Ding, E. Y., Smith, J. M. and Miyamoto, S., Hexokinase-II positively regulates glucose starvation-induced autophagy through TORC1 inhibition. *Mol. Cell* 2014. 53: 521–533.
- 29 Kishore, M., Cheung, K. C. P., Fu, H., Bonacina, F., Wang, G., Coe, D., Ward, E. J. et al., Regulatory T cell migration is dependent on glucokinase-mediated glycolysis. *Immunity* 2017. 47: 875–889.e10.
- 30 Roberts, D. J. and Miyamoto, S., Hexokinase II integrates energy metabolism and cellular protection: Acting on mitochondria and TORC1 to autophagy. *Cell Death Differ.* 2015. 22: 248–257.
- 31 Ciscato, F., Ferrone, L., Masgras, I., Laquatra, C. and Rasola, A., Hexokinase 2 in cancer: a prima donna playing multiple characters. *Int. J. Mol. Sci.* 2021. 22: 4716.
- 32 Bryan, N. and Raisch, K. P., Identification of a mitochondrial-binding site on the N-terminal end of hexokinase II. *Biosci. Rep.* 2015. 35: e02025.
- 33 Shangguan, X., He, J., Ma, Z., Zhang, W., Ji, Y., Shen, K., Yue, Z. et al., SUMOylation controls the binding of hexokinase 2 to mitochondria and protects against prostate cancer tumorigenesis. *Nat. Commun.* 2021. 12: 1812.
- 34 Taylor, R. C., Cullen, S. P. and Martin, S. J., Apoptosis: controlled demolition at the cellular level. *Nat. Rev. Mol. Cell Biol.* 2008. 9: 231–241.
- 35 Mathupala, S. P., Ko, Y. H. and Pedersen, P. L., Hexokinase II: cancer's double-edged sword acting as both facilitator and gatekeeper of malignancy when bound to mitochondria. *Oncogene* 2006. 25: 4777–4786.
- 36 Gong, L., Cui, Z., Chen, P., Han, H., Peng, J. and Leng, X., Reduced survival of patients with hepatocellular carcinoma expressing hexokinase II. *Med. Oncol.* 2012; 29: 909–914.
- 37 Lis, P., Dyląg, M., Niedźwiecka, K., Ko, Y. H., Pedersen, P. L., Goffeau, A. and Ułaszewski, S., The HK2 dependent 'Warburg Effect' and mitochondrial oxidative phosphorylation in cancer: targets for effective therapy with 3-bromopyruvate. *Molecules* 2016. 21: 1730.
- 38 Kooshki, L., Mahdavi, P., Fakhri, S., Akkol, E. K. and Khan, H., Targeting lactate metabolism and glycolytic pathways in the tumor microenvironment by natural products: A promising strategy in combating cancer. *Biofactors* 2022. 48: 359–383.
- 39 Pastorino, J. G. and Hoek, J. B., Hexokinase II: the integration of energy metabolism and control of apoptosis. *Curr. Med. Chem.* 2003. 10: 1535–1551.
- 40 Sugiyama, T., Shimizu, S., Matsuoka, Y., Yoneda, Y. and Tsujimoto, Y., Activation of mitochondrial voltage-dependent anion channel by proapoptotic BH3-only protein Bim. *Oncogene* 2002. 21: 4944–4956.
- 41 Marquardt, J. U. and Edlich, F., Predisposition to apoptosis in hepatocellular carcinoma: from mechanistic insights to therapeutic strategies. *Front. Oncol.* 2019. 9: 1421. Available at: <https://www.frontiersin.org/articles/10.3389/fonc.2019.01421>
- 42 Schoeniger, A., Wolf, P. and Edlich, F., How do hexokinases inhibit receptor-mediated apoptosis? *Biology* 2022. 11: 412.
- 43 Lauterwasser, J., Fimm-Todt, F., Oelgeklaus, A., Schreiner, A., Funk, K., Falquez-Medina, H., Klesse, R. et al., Hexokinases inhibit death receptor-dependent apoptosis on the mitochondria. *Proc. Natl. Acad. Sci. U. S. A.* 2021. 118: e2021175118.
- 44 Yin, X.-M., Wang, K., Gross, A., Zhao, Y., Zinkel, S., Klocke, B., Roth, K. A. et al., Bid-deficient mice are resistant to Fas-induced hepatocellular apoptosis. *Nature* 1999. 400: 886–891.
- 45 Zhao, Y., Ding, W., Qian, T., Watkins, S., Lemasters, J. J. and Yin, X., Bid activates multiple mitochondrial apoptotic mechanisms in primary hepatocytes after death receptor engagement. *Gastroenterology* 2003. 125: 854–867.
- 46 Wei, M. C., Lindsten, T., Mootha, V. K., Weiler, S., Gross, A., Ashiya, M., Thompson, C. B. et al., tBID, a membrane-targeted death ligand, oligomerizes BAK to release cytochrome c. *Genes Dev.* 2000. 14: 2060–2071.
- 47 Zheng, M., Wu, C., Yang, K., Yang, Y., Liu, Y., Gao, S., Wang, Q. et al., Novel selective hexokinase 2 inhibitor Benitrobenzamide blocks cancer cells growth by targeting glycolysis. *Pharmacol. Res.* 2021. 164: 105367.
- 48 Rual, J.-F., Hirozane-Kishikawa, T., Hao, T., Bertin, N., Li, S., Dricot, A., Li, N. et al., Human ORFeome version 1.1: a platform for reverse proteomics. *Genome Res.* 2004. 14: 2128–2135.
- 49 Hayek, S., Bekaddour, N., Besson, L., Alves de Sousa, R., Pietrancosta, N., Viel, S., Smith, N. et al., Identification of primary natural killer cell modulators by chemical library screening with a luciferase-based functional assay. *SLAS Discov.* 2019. 24: 25–37.
- 50 Cossarizza, A., Chang, H.-D., Radbruch, A., Abrignani, S., Addo, R., Akdis, M., Andrä, I. et al., Guidelines for the use of flow cytometry and cell sorting in immunological studies (third edition). *Eur. J. Immunol.* 2021. 51: 2708–3145.

Abbreviations: **G6P:** glucose-6-phosphate · **GCK:** glucokinase · **HCC:** hepatocellular carcinoma · **HK:** hexokinases · **ILCs:** innate lymphoid cells · **NK:** natural killer · **OXPHOS:** oxidative phosphorylation · **tBID:** truncated BID · **VDAC:** voltage-dependent anion channel

Full correspondence: Dr. Laure Perrin-Cocon, CIRI – VIRIMI Team, 21 av. Tony Garnier, 69365 Lyon Cedex, France
e-mail: laure.perrin@inserm.fr

Received: 13/12/2023

Revised: 27/5/2024

Accepted: 28/5/2024

Accepted article online: 29/5/2024